Carbohydrate Polymers 82 (2010) 786–794

Contents lists available at ScienceDirect

Carbohydrate Polymers

journal homepage: www.elsevier.com/locate/carbpol

Iodine absorption properties and its effect on the crystallinity of developing wheat starch granules

R.N. Waduge[a], S. Xu[b], K. Seetharaman[a,*]

[a] Department of Food Science, University of Guelph, Guelph, ON, N1G 2W1, Canada
[b] Applications Scientist, Agilent Technologies

ARTICLE INFO

Article history:
Received 3 April 2010
Received in revised form 8 May 2010
Accepted 26 May 2010
Available online 4 June 2010

Keywords:
Starch
Premature starch
Granule architecture
Iodine
WAXS
K/S spectra
AFM

ABSTRACT

Wheat starches at different stages of maturities were evaluated for their iodine absorption properties by measuring the ratio of absorption to reflection spectra (K/S) and crystalline structure by using wide angle X-ray scattering (WAXS). The surface of starch granules was also visualized by using atomic force microscopy (AFM). The K/S spectral data demonstrated different levels of mobility of starch polymers at different stages of maturity and the mobility of longer chain polymers with increasing moisture contents. Iodine did not change the characteristic A-type crystalline pattern. However, the extent of effect of iodine on starch crystallinity was affected by maturity and moisture content of starches. AFM images of iodine exposed starches supported the interaction of iodine molecules with starch polymers. Differences in surface features were observed for different maturities.

1. Introduction

In mature wheat endosperm, there are two distinct populations of starch granules: large disc-shaped A-granules and small spherical-shaped B-granules (Peng, Gao, Abdel-Aal, Hucl, & Chibbar, 1999). The granules of different sizes and shapes are initiated in the endosperm during different stages of grain development. Large granules appear at about 4–7 DAA (days after anthesis) and continue to increase in size throughout the grain filling period, while small granules are initiated at about 12–14 DAA and remain considerably small at final maturity (Bechtel & Wilson, 2003; Bechtel, Zayas, Kaleikau, & Pomeranz, 1990; Langeveld, Van Wijk, Stuurman, Kijne, & de Pater, 2000). At maturity, A-granules have an average diameter of 10–35 μm and B-granules range from 1 to 10 μm average diameter. Starch granules are mainly composed of two types of glucose polymers—amylose (AM), which is essentially a linear chain molecule, and amylopectin (AMP), which is branched. The AM content in starches of wheat and barley increases during grain development (Kulp & Mattern, 1973; McDonald, Stark, Morrison, & Ellis, 1991; Morrison & Gadan, 1987) and at all maturities, the AM content of A-type granules is higher than in B-type granules (McDonald et al., 1991; Morrison & Gadan, 1987). In the semicrystalline starch granule, these polymers are packed in a pattern such that branch chain polymers of AMP forms double helices, and occupy the crystalline area of the granule, while AMP branch points and AM are located in the amorphous area of the granule. The currently accepted model to describe the semicrystalline structure of the starch granule is the "Blocklet model" (Gallant, Bouchet, & Baldwin, 1997). This model is supported by studies carried out by using AFM (Baldwin, Adler, Davies, & Melia, 1998; Baldwin, Davies, & Melia, 1997; Juszczak, Fortuna, & Krok, 2003a, 2003b).

Iodine binds with linear glucan polymers of starch forming an inclusion complex. The structure of iodine–linear glucan polymer complex in non-granular condition is well known (Bates, French, & Rundle, 1943; Gessler et al., 1999; Hayashi, Kiribuchi-Otobe, & Seguchi, 2005; Kuntson, Cluskey, & Dintzis (1982); Murdoch, 1992; Nimz et al., 2003; Rundle & Baldwin, 1943; Rundle & Edwards, 1943; Rundle & French, 1943a, 1943b; Teitelbaum, Ruby, & Marks, 1980; Thoma & French, 1960). The color and wavelength of the maximum absorbance of the complex vary according to the degree of polymerization (DP) of the polymer chain (Banks, Greenwood, & Khan, 1971). The reaction of iodine with linear polymers of starch is widely used for determining the AM content of starches. However, Saibene and Seetharaman (2006) used iodine to study the architecture of the starch granule for the first time. They observed that at moisture contents between 12 and 20%, iodine was able to form complexes with linear polymers and disrupt the crystalline arrangement of starch polymers within the granule. Rendleman

* Corresponding author. Tel.: +1 519 824 4120x52204; fax: +1 519 824 6631.
E-mail addresses: rwaduge@uoguelph.ca (R.N. Waduge), kseethar@uoguelph.ca (K. Seetharaman).

0144-8617/$ – see front matter © 2010 Published by Elsevier Ltd.
doi:10.1016/j.carbpol.2010.05.053

(2003) reported that the source of iodine ion in this system comes from the hydrolysis of molecular iodine by water of hydration in the starch. This was supported by Saibene, Zobel, Thompson, and Seetharaman (2008) who reported higher iodine binding in corn starch than in potato starch under controlled moisture contents of 12–20%. They further observed a greater effect of iodine on the crystallinity of potato starch than that of corn starch. The interaction of iodine vapor with native granular starch is likely a surface reaction. Since the starch in this experimental system is in its granular form, the formation of inclusion complexes with iodine vapor depends on the accessibility of segments of glucan polymers, i.e., segments of AM molecules which are not trapped in the crystalline lamellae or those that are not in the double helices with AMP branch chains; or longer segments of AMP branch chains, to iodine. Therefore, the ability of iodine to bind depends on the organization of linear glucan polymers within the granule. The ability of iodine molecules to penetrate the starch granule also likely depends on the surface features of the granule such as pores or penetrating channels. Existence of pores and channels on the surface of wheat starch granules has been reported (Kim and Huber, 2008).

Complex formation of iodine with granular starch has been studied by using K/S spectra (Saibene & Seetharaman, 2006; Saibene et al., 2008) and WAXS (Rendleman, 2003; Saibene & Seetharaman, 2006; Saibene et al., 2008). K/S spectra gives information about the intensity of the color developed in granular starch when it is bound with iodine, while WAXS is used to measure the effect of iodine binding to the crystallinity of the granule. AFM has been used to study the starch granule surface (Ayoub, Ohtani, & Sugiyama, 2006; Baldwin et al., 1997; Juszczak, 2003; Juszczak et al., 2003a; Ohtani, Yoshino, Ushiki, Hagiwara, & Maekawa, 2000), internal structure of the granule (Baker, Miles, & Helbert, 2001; Ridout, Gunning, Parker, Wilson, & Morris, 2002; Ridout, Parker, Hedley, Bogracheva, & Morris, 2004; Szymonska & Krok, 2003), starch components (Dang, Braet, & Copeland, 2006; Gunning et al., 2002; Liu et al., 2001), enzymatic degradation of starch granule (Morris, Gunning, Faulds, Williamson, & Svensson, 2005; Thomson, Miles, Ring, Shewry, & Tatham, 1994), retrogradation (Tang & Copeland, 2007), and gelatinization (An, Yang, Liu, & Zhang, 2008).

The objective of this research was to probe the molecular organization of wheat starch granules at different stages of maturity by studying their iodine binding properties and its effect on the crystallinity of starch granules.

2. Materials and methods

2.1. Materials

Hard red spring wheat at three different maturities – 17, 28, and 47 days after pollination (DAP) – were harvested in Elora, Ontario, Canada in 2008. Grains were sampled directly from the field and stored at −20 °C to prevent any enzyme activity. All chemicals used were in ACS certified grade.

2.2. Starch isolation

Starches were isolated according to the method of Park, Bean, Wilson, and Schober (2006) with some modifications. 100 g of the grain was frozen in liquid nitrogen and ground in a coffee grinder for 1 min. The resulting flour was stirred with sodium borate buffer (12.5 mM, pH 10, containing 0.5% SDS (w/v) and 0.5% $Na_2S_2O_5$ (w/v)) for 5 min, transferd into 280 mL centrifuge bottles, and the residue was recovered by centrifugation at 900 × *g* for 5 min. These three steps were repeated once again. The residue was washed once with distilled water, neutralized with 0.01 M HCl and recovered by centrifugation. Then the residue was suspended in distilled water, passed through four layers of cheesecloth and then through 70 μm nylon mesh (step A). The resulting residue was stirred overnight with water to recover any remaining starch while the purification process was continued with the slurry. The slurry was centrifuged and the brown layer, formed on the top of the starch layer, was scraped using a spatula and transferred into a beaker. Then the starch was suspended again in water and centrifuged in 50 mL centrifuge tubes at 1600 × *g* for 10 min. These steps were continued until all the brown particles were removed from the starch fraction. All the brown fractions were combined in a beaker. Starch granules mixed with the brown layer were recovered by gravity settling and added back to the purified starch fraction. The residue which was stirred overnight was continued as from step A. The purified starch was washed once with acetone and air dried. Amylose content of starches was determined using the method described by Chrastil (1987) and was 17.4, 23.2, and 23.2% for 17, 28, and 47 DAP starches, respectively. The nitrogen content of all starches was less than 0.05% as determined by using Dumas combustion method (Leco EP 528, Leco Instruments Ltd. Canada) (Simonne, Simonne, Eitenmiller, Mills, & Cresman, 1997).

2.3. Sample preparation

Starches were equilibrated to 0.33, 0.75 or 0.97 water activity (a_w) in desiccators containing saturated solutions of $MgCl_2$, NaCl, and K_2SO_4, respectively, at room temperature. The final equilibrated moisture contents were about 11, 15.5, and 20% at 0.33, 0.75, and 0.97a_w, respectively. Equilibrated starches (0.2 g) were spread over a plastic weighing pan and exposed to iodine vapor generated from 2 g of iodine crystals placed in a desiccator at the corresponding water activity for 24 h at room temperature (Saibene & Seetharaman, 2006). Fresh samples were prepared for each experiment.

2.4. Colorimetric analysis

The color (L^* (white/black), a^* (green/red), and b^* (blue/yellow)) and the K/S value of starch–iodine complex were evaluated by using CM 3500-d spectrophotometer (Konica Minolta Sensing Inc., Mahwah, NJ, USA) equipped with SpectraMagic NX CM-S 100 software. Measurements were taken over a wavelength range from 400 to 700 nm and using starch which was equilibrated to the same a_w but not exposed to iodine vapor as the reference. The granular starch (0.2 g) was spread over the sample cell as a thick layer and the measurements were taken. The K/S, which was derived by Kubelta and Munk, is defined as follows:

$$\frac{K}{S} = \frac{(1-R)^2}{2R}$$

where K is the absorption coefficient, S is the scattering coefficient, and R is the reflectance of the sample expressed as a fraction between 0 and 1 (Billmeyer & Saltzman, 1981).

2.5. WAXS analysis

X-ray diffractograms were obtained for starches, packed tightly into a 1 in. × 1 in. square shape area of a quartz plate, by using the radiation produced by the copper ($K\alpha_1$ = 0.154 nm) X-ray tube in the Rigaku X-ray diffractometer (Rigaku-Denki, Co., Tokyo, Japan). The operating conditions were as follows: target voltage 40 kV, current 40 mA, scan speed 1°/min, sampling width 0.02°, divergence slit width 0.5°, scatter slit width 0.5°, receiving slit width 0.3 nm, and scanning range 3–35°. Data were smoothed using Jade software (version 6.5, Material Data Inc., California, USA) and normalized to equal total scattering in 3–35° 2θ range. Peak width at half height (PWHH) and percentage relative crystallinity (%RC) were

calculated by using the curve fitting procedure described by Lopez-Rubio, Flanagan, Gilbert, and Gidley (2008) using Igor Pro software (version 6.0.5.0, WaveMetrics Inc. Oregon, USA). The PWHH was calculated after subtracting the amorphous background. Only the finger print peaks (15°, 17°, 18°, 20°, and 23° 2θ) were considered for the %RC calculation. Eqs. (1) and (2) were used to calculate %RC and the percentage difference in PWHH (%Diff. in PWHH), respectively.

$$\%RC = \frac{\sum_{k=1}^{n} A_{Ck}}{\sum_{k=1}^{n} A_{Ck} + A_a} \times 100 \quad (1)$$

where A_{Ck} is the area under each crystalline peak with index k and A_a is the area under the amorphous peak.

$$\%\text{Diff. in PWHH} = \frac{\text{PWHH (Starch} + I_2) - \text{PWHH (Starch)}}{\text{PWHH (Starch)}} \times 100 \quad (2)$$

where PWHH (starch + I_2) is the peak width of iodine exposed starch and PWHH (starch) is the peak width of control starch.

Percentage V-crystallinity (%RC_V) was calculated by dividing the area under the peak at 20° 2θ over the total area of the diffractogram. Percentage A-crystallinity (%RC_A) was calculated by taking the difference of %RC and %RC_V.

2.6. AFM analysis

AFM analysis was performed with the Agilent Technologies model 5500 instrument (UPPSALA, Sweden). All images were obtained with silicon cantilevers with nominal spring constant of 48 N/m and resonance frequency of around 300 kHz (Nanoworld AG, Switzerland). Scanning rates were typically 1–2 Hz. Images of the starch surface were mostly acquired with AC mode at a slightly repulsive force region of the tip-sample distance, however, images of the very soft polymer brush protrusions were acquired at attractive force region with low cantilever oscillation amplitude of around 1–2 nm with low scanning speed of around 0.5 Hz. The observation was performed inside a chamber at room temperature. Starch granules were spread over a double-sided tape on a microscopic slide without any preliminary preparations. The exposed surface of the starch was placed on the sample holder and the image was directly scanned from the granule surface.

3. Results and discussion

3.1. Color development in iodine exposed starches

Photographs of starches from three different maturities which are exposed to iodine vapor following equilibration to 0.33, 0.75, and 0.97a_w are shown in Fig. 1. The change in color of samples is evident with increasing moisture content. Differences between color intensities of starches from different maturities were visible at lower moisture contents. However, the color development of starches which were equilibrated to 0.97a_w was too intense to visualize any difference between them. Furthermore, color intensity measurements which are taken by the spectrophotometer (L^*, a^*, and b^*) for the same set of starches are shown in Fig. 2. As seen in Fig. 2a, L^* was not significantly different between starches from different maturities which were equilibrated to the same a_w. However, increasing moisture content decreased L^* of each starch indicating the color shift from white to black. The decrease in a^* followed the order of 0.75 > 0.97 > 0.33a_w in starches of all three

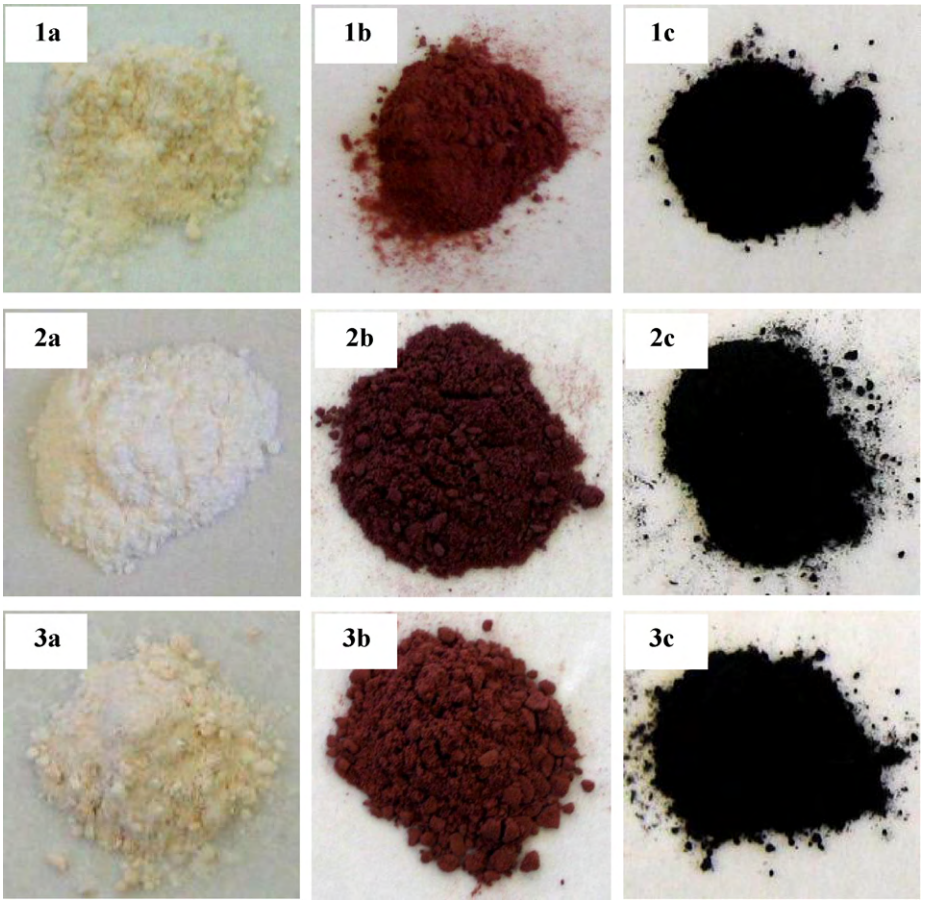

Fig. 1. Photographs of starches exposed to iodine following equilibration to different a_w. (a) 0.33a_w, (b) 0.75a_w, (c) 0.97a_w, (1) 17 DAP, (2) 28 DAP, and (3) 47 DAP.

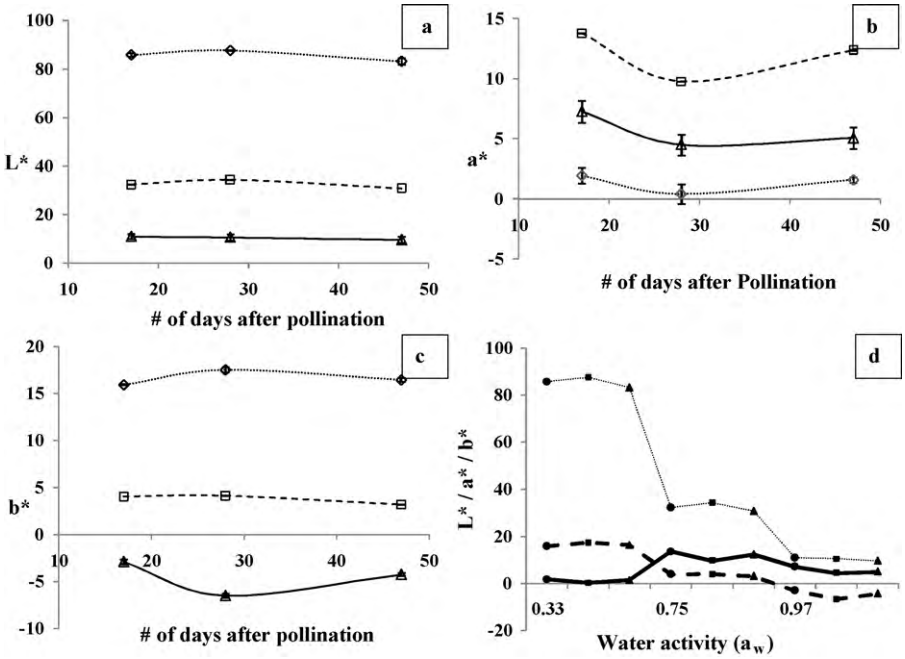

Fig. 2. Color development of starches exposed to iodine following equilibration to different a_w. (a), (b), and (c) show L^* value (white/black), a^* value (green/red), and b^* value (blue/yellow), respectively, as a function of maturity; (◊) 0.33, (□) 0.75, and (Δ) 0.97a_w. (d) shows the comparison of L^* (·····), a^* (—), and b^* (——) values of iodine exposed starches of 17 DAP (●), 28 DAP (■), and 47 DAP (▲) as a function of a_w.

maturities (Fig. 2b). Furthermore, a^* of 28 DAP starch was lower than other two starches at all moisture contents indicating its low intensity in the red spectrum. Furthermore, the b^* of all three starches was decreased with increasing moisture content (Fig. 2c). At 0.97a_w, 28 DAP starch showed the minimum b^* indicating highest intensity in blue spectrum, while it is slightly lower than other two starches at lower moisture contents. However, this difference was not observable visually. L^*, a^*, and b^* as function of a_w is shown in Fig. 2(d).

3.2. K/S spectral analysis

Starches were studied as populations of mixed large and small granules. K/S spectra of three iodine exposed starches (17 DAP, 28 DAP, and 47 DAP) following equilibration to 0.33, 0.75 and 0.97a_w were measured. Fig. 3 shows data obtained for starches equilibrated to 0.75 and 0.97a_w. Increasing moisture content increased the intensity of the color developed in the starches at all three maturities. A similar effect had been observed for mature potato and corn starches (Saibene & Seetharaman, 2006; Saibene et al., 2008). At all three maturities, starches which were equilibrated to 0.33a_w did not show a peak K/S maxima (data not shown). However, starches equilibrated to 0.75a_w exhibited multiple maxima values (λ_{max}) as 520, 530, and 530 nm for 17, 28 and 47 DAP starches, respectively. The intensity of the color developed in 28 DAP starch was always lower than that of the other two starches, while the 47 DAP starch showed the highest K/S at all wavelengths (Fig. 3a). This was further visualized by the color development of starches equilibrated to 0.75a_w which demonstrated that 28 DAP starch has the highest L^* and lowest a^* compared to its other counterparts while 47 DAP starch has the lowest L^* and b^* compared to its other counterparts (Fig. 2d). This suggests that at 0.75a_w, the population of glucan polymers available to form inclusion complexes with iodine in 28 DAP starch is lower than that of 17 DAP starch indicating different molecular organizations at different stages of maturity. Furthermore, Starches equilibrated to 0.97a_w had the following trend for the K/S maxima: 17 DAP < 28 DAP ~ 47 DAP (Fig. 3b) demonstrating

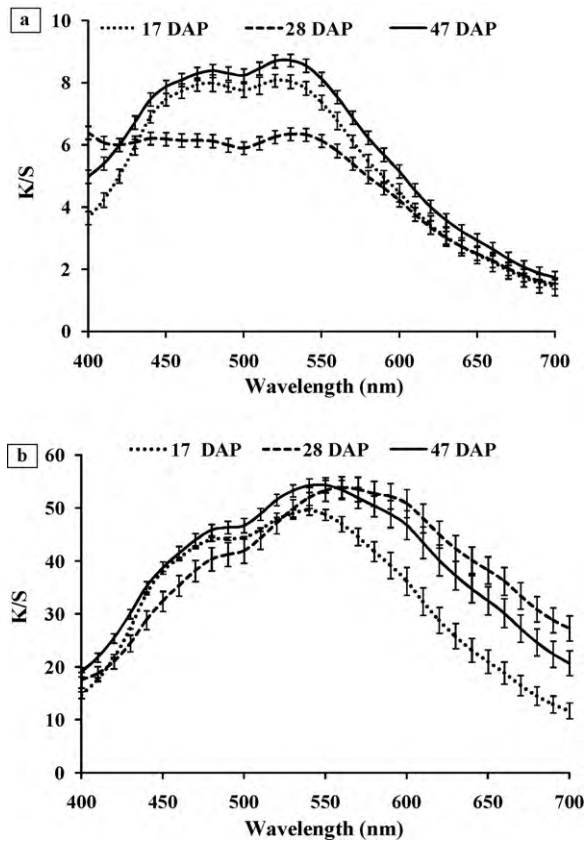

Fig. 3. Absorption spectra of 17 DAP (·····), 28 DAP (——), and 47 DAP (—) iodine-exposed starches following equilibration to (a) 0.75a_w, and (b) 0.97a_w. K/S is the ratio of absorption/scattering coefficients.

Table 1
Degree of polymerization (DP) of starch linear polymer chains that are likely mobile and complexed with iodine at 0.75 or 0.97a_w at different stages of maturity.

Maturity level	0.75a_w		0.97a_w	
	λ_{max} (nm)	DP[a]	λ_{max} (nm)	DP[a]
17 DAP	520	28.1	540	34.9
28 DAP	530	31.1	560	45.0
47 DAP	530	31.1	550	39.4

[a] Values represents the mean of three determinations and were extrapolated from Banks et al. (1971).

the availability of more glucan polymers in 28 DAP starch to interact with iodine vapor at higher moisture contents than that in 17 DAP starch. This suggests that it is not just the presence of glucan polymers in the starch granule that determines the level of interaction with iodine, but their ability to form the single helices in the presence of iodine. Since glucan polymers are in their rubbery state at 0.97a_w, there will be longer as well as higher population of glucan polymers that can form inclusion complexes with iodine. The λ_{max} were 540, 560, and 550 nm for 17, 28 and 47 DAP starches, respectively. In addition, at wavelengths higher than λ_{max}, 28 DAP starch showed higher K/S values than the 47 DAP starch when equilibrated to 0.97a_w, while this effect was not observed in starches equilibrated to 0.75a_w. This indicates that at 0.97a_w, 28 DAP starch has a higher population of longer segments of starch polymers which is mobile and can form complexes with iodine than other two maturities.

The likely degree of polymerization of the linear polymers at the corresponding K/S maxima for the starches is listed in Table 1, based on the calculations by Banks et al. (1971) for solution systems. The length of glucan polymers determines the color and absorbance values of the starch–iodine complex in dispersed systems (Banks et al., 1971). In granular starches, we have demonstrated that, it is the mobility of glucan polymers that determines the extent of complex formation with iodine, but not directly the amount of amylose or amylopectin present (unpublished data; manuscript in review). Furthermore, Teitelbaum et al. (1980) have shown that starch–iodine complex formed by granular starch and iodine vapor are not different from the complex formed in solutions, using Mössbauer spectroscopy. Therefore, we believe that it is reasonable to use Banks et al.'s calculation to determine the length of glucan polymers that are mobile in granular starches to form starch–iodine inclusion complex with iodine at that specific a_w.

Different behaviors of starches from different maturities at the same moisture content together with the same starch at different moisture contents demonstrate differences in their molecular organizations during maturity. Compared to the K/S spectral data obtained for corn starches by Saibene and Seetharaman (2006), in our observations, wheat starch exhibited lower K/S values at all corresponding a_w values, although both corn and wheat have similar A-type crystallinity. Furthermore, these researchers have reported K/S maxima for corn starches at water activity as low as 0.33, while in our study K/S maxima was only observed for wheat starches equilibrated to 0.75a_w. On the other hand, potato starch, which has the B-type crystallinity, did not exhibit K/S maxima below 0.97a_w (Saibene & Seetharaman, 2006). Sevenou and coworkers have demonstrated that external regions of potato starch granules are more ordered than that of corn or wheat starch granules using Fourier transform infrared spectroscopy (Sevenou, Hill, Farhat, & Mitchell, 2002). Therefore, it is likely that wheat and corn starch granules have less tighter packing compared to potato starch, such that the external polymers likely have higher mobility of at a specific a_w. Similarly, the differences observed in K/S spectra of starches from different maturities and at different moisture contents could be attributed to different packing arrangements of starch polymers within the granule.

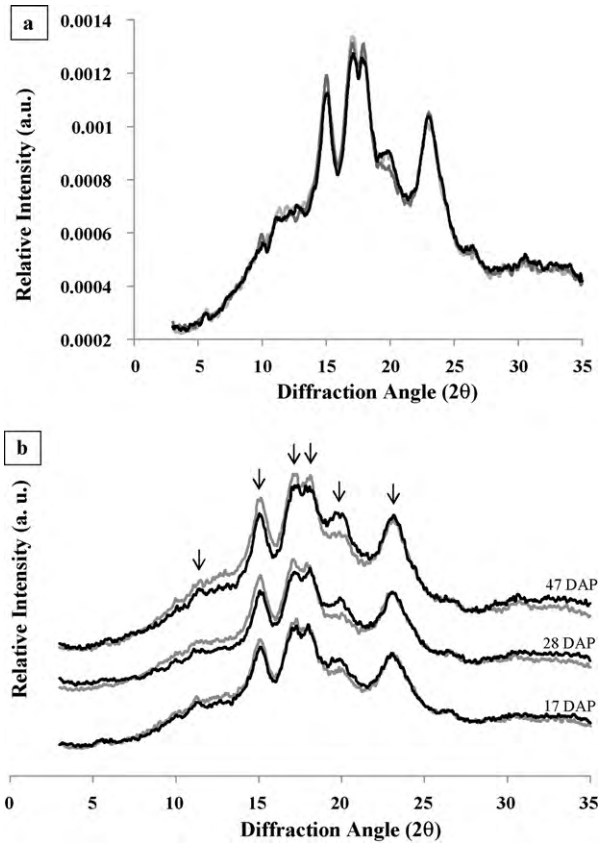

Fig. 4. X-ray powder diffraction pattern of 17, 28, and 47 DAP starches, following equilibration to 0.97a_w. (a) Effect of the maturity; increased color intensity of diffractograms represent the increased maturity. (b) Effect of iodine exposure; light color represent the control starch while dark color represents the iodine exposed starch; arrows highlight fingerprint peaks of X-ray diffractograms that has been affected by iodine; the graphs are offset for clarity.

3.3. WAXS analysis

X-ray diffractograms of wheat starches of three different maturities equilibrated to 0.97a_w are shown in Fig. 4a. Starches from all three maturities showed the characteristic A-type X-ray pattern. This suggests that organization of starch polymers into the A-type polymorphic structure of wheat starch is established at very early stages of the granule development and does not change during maturity. This is supported by previous studies carried out with potato (Liu, Weber, Currie, & Yada, 2003), water caltrop (Chiang, Li, Huang, & Wang, 2007), and soybean (Stevenson, Jane, & Inglett, 2007) starches which exhibited unchanged B-type, A-type, and C_B-type polymorphic structures, respectively, during their maturity. Furthermore, there were no differences between peak positions of starches of different maturities whereas, small differences were observed in intensities of all fingerprint peaks (15°, 17°, 18°, 20° and 23° 2θ). Minor differences in peak intensities have been observed in potato (Liu et al., 2003) and water caltrop (Chiang et al., 2007) starches also. The 20° 2θ peak, which is the peak responsible for V-type crystallites, demonstrated the following trend in peak intensity: 28 DAP < 17 DAP ~ 47 DAP. Morrison and Gadan (1987) have reported that the lipid content of wheat starch increase during maturity. Furthermore, the X-ray peak at 20° 2θ is only indicative of V-crystallites which was organized into an ordered array (Morrison, 1988). Therefore, according to our observations with X-

ray diffractograms that shows less V-type crystallites in 28 DAP starch than starches from the other two maturities, it is likely that although 28 DAP starch has more lipids than 17 DAP starch, not all of them were complexed with starch polymers in its native state or they were complexed with starch polymers but were not organized into an ordered structure reflected by X-ray crystallinity. Morrison (1988) has reported that lipid–amylose complexes can only form at elevated temperatures. Since the experiments were carried out at room temperature, it is likely that starch-iodine complex formation is not influenced by lipids present in the native starch.

Fig. 4b shows the effect of iodine exposure to the polymorphic pattern and the crystallinity of starches at the three different maturities following equilibration to 0.97a_w. Iodine did not change the polymorphic pattern of starches of all three maturities. The same behavior had previously observed by Cheetham and Tao (1998) for mature maize starches of different amylose contents and for mature potato starch even when they were exposed to iodine vapor for 4 months. The formation of iodine–glucan complex, when granular starches of three different maturities are exposed to iodine vapor, affected the crystallinity of starches to different extents depending on their moisture content. While there was no effect of iodine exposure on the X-ray diffractograms of starches equilibrated to 0.33a_w, iodine exposure slightly changed the intensity of finger print peaks in starches from all three maturities when equilibrated to 0.75a_w (data not shown). The effect of iodine binding on the crystallinity of starches was strong and clearly visible in starches equilibrated to 0.97a_w (Fig. 4b). At this a_w, peak positions were not changed; however, iodine decreased the intensity of peaks at around 15°, 17°, and 18° 2θ and increased the intensity of peaks at around 20° and 23° 2θ. Furthermore, the increased peak intensity at around 23° 2θ was only marginally. This effect was more pronounced with the increasing maturity of starch. Previously, Saibene et al. (2008) have reported a decrease in the intensity of peaks at around 15°, 17°, 18° and 23° 2θ in corn starch and a loss of resolution in peaks at around 23° and 24° 2θ in potato starch, when they were equilibrated to 0.97a_w and were exposed to iodine. Cheetham and Tao (1998) reported that iodine vapor exposure decreased peak intensities in normal maize starches whereas, some peaks dissapeared in high amylose maize starch. The above report lend credence to our results.

Percentage relative crystallinity (%RC) of A-type crystallites (%RC_A) and V-type crystallites (%RC_V), as well as peak widths at half height (PWHH) in diffractograms were calculated using the curve fitting technique. A Gaussian fitting was used. Fig. 5a shows the effect of iodine on %RC_A and %RC_V of starches of all three maturities. Typically, %RC is calculated by dividing the area under crystalline peaks by the total area under the diffractogram. Therefore, the %RC is a combination of %RC_A and %RC_V for cereal starches. However, this traditional method of calculating %RC does not provide a meaningful interpretation for samples exposed to iodine, due to the formation of V-crystallites reflected at 20° 2θ. Therefore, in this study A-crystallinity and V-crystallinity were calculated individually. "A-crystallinity" is the crystallinity that comes from AMP double helices and "V-crystallinity" is the crystallinity that comes from V-crystallites that is formed by starch-lipid and/or starch–iodine inclusion complexes (Buleon, Veronese, & Putaux, 2007). As expected, %RC_V increased when starches were exposed to iodine (Fig. 5a). %RC_A of 17 DAP and 28 DAP starches were decreased while that of 47 DAP starch was slightly increased due to the iodine exposure. Although there were differences in the level of the effect, no relationship between maturities could be found. Furthermore, the different behavior of 28 DAP starch could also be seen. PWHH of all finger print peaks of all three maturities, except peaks at around 17° and 20° 2θ, were decreased by the interaction with iodine whereas, that of latter two peaks were increased (Fig. 5b). However, the increase in the width of the peak at around 20° 2θ was more pronounced compared to that of the peak at 17° 2θ. Iodine also increased the area of peaks at around 10° and 13° 2θ, indicating the increased contribution from single helices to the crystallinity of the starch granule.

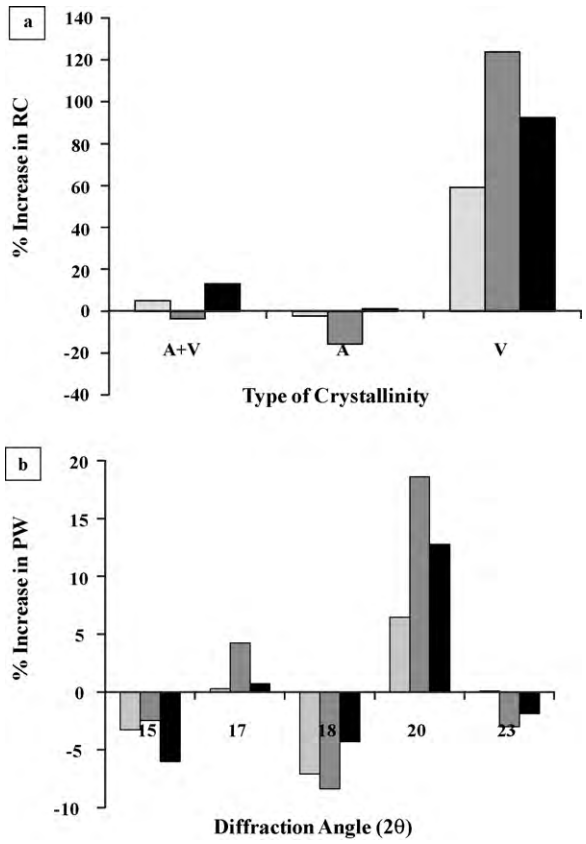

Fig. 5. Effect of iodine on the crystallinity (a), and the peak width at half height (b) of starches equilibrated to 0.97a_w; increasing color intensity represents the increasing maturity. In figure (a), %RC_A denotes the percentage difference in A-crystallinity and %RC_V denotes the percentage difference in V-crystallinity. In figure (b) percentage increase in PWHH was calculated using the equation: % Diff = [(width of iodine-exposed starch − width of control starch)/width of control starch] × 100.

In X-ray diffractograms, the peak intensity measures the amount of ordered crystallites, while the peak width measures the crystallite perfection; i.e., the crystallite size (Suryanarayana & Norton, 1998). Accordingly, changes in intensities and widths of peaks at around 15°, 17°, 18° and 23° 2θ in X-ray diffractograms of wheat starches of three different maturities discussed above, most likely represent the disruption of A-type crystallites which was in the boundary of order/disorder into completely disorder/amorphous state. Therefore, the starch samples likely have relatively more ordered, but lower amount of crystallites. This is further confirmed by the observed %RC_A reduction when the starch was exposed to iodine (Fig. 5a). Furthermore, the increased peak intensity at around 20° 2θ is due to starch-iodine complex formation. The increased PWHH of the peak at around 20° 2θ can be attributed to the disruption of V-type crystallites which was already in the starch and/or formation of less ordered crystallites by iodine. The formation of iodine–glucan complex was evident in the color intensity measurements, photographs and K/S spectra of starches.

Linear polymers or linear segments of branched polymers have the ability to bind with iodine. Although the AM content of wheat starch was increased during grain development, it is the mobility of these polymers that is the determining factor in iodine binding of native granular starches (Saibene & Seetharaman, 2006). The mobility of starch polymers is determined not by the amount of either AM or AMP, but rather by the architecture, i.e., the organi-

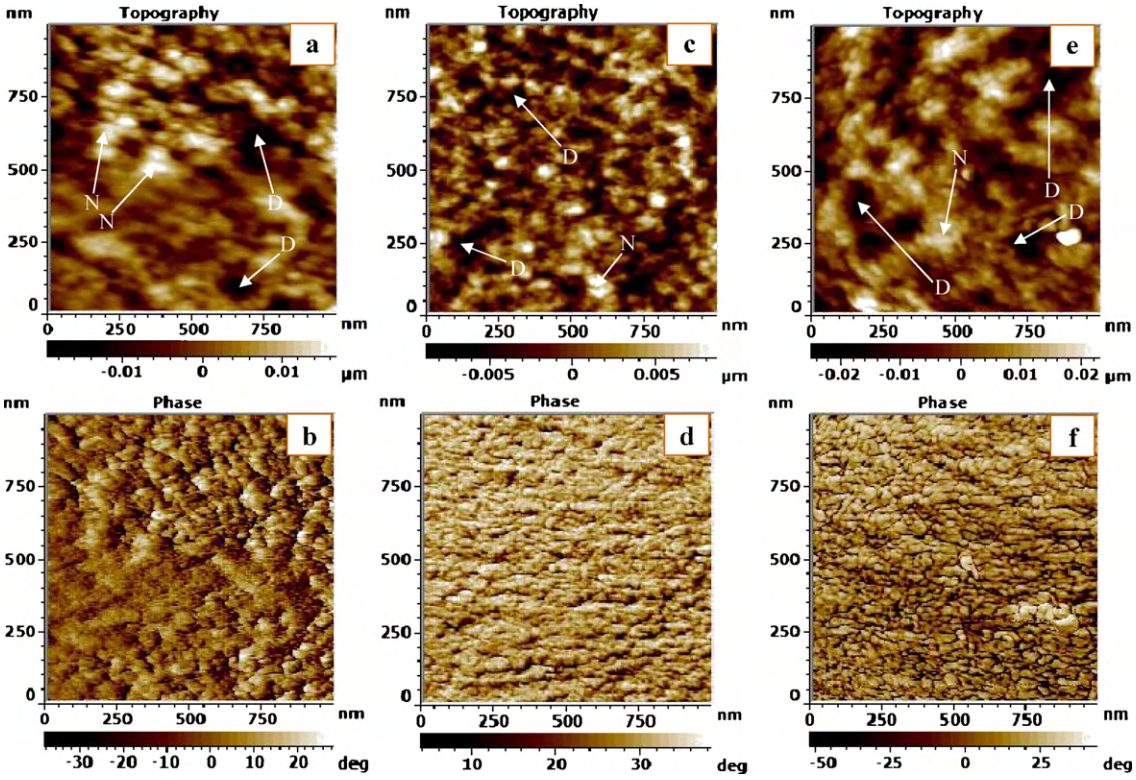

Fig. 6. Topographic and phase AFM images of the surface of native starch granules of different maturities equilibrated to 0.97a_w. (a) 17 DAP, topographic; (b) 17 DAP, phase; (c) 28 DAP, topographic; (d) 28 DAP, phase; (e) 47 DAP, topographic; (f) 47 DAP, phase. The scan size is 1 μm × 1 μm. Depressions are shown by arrows labelled as 'D' and nodules are shown by arrows labelled as 'N'.

zation of these polymers within the granule. Therefore, differences shown by the starches of varying maturity with respect to peak intensity and peak width reflected differences in the organization of AM and/or AMP within the granule interior.

3.4. AFM analysis

Surfaces of randomly selected starch granules from three different maturities were studied using AFM (Fig. 6). Several granules were imaged before selecting one that is presented. While it is not easy to identify if the image presented is from a large or small granule, the overall observations were evident on all granule surfaces imaged. Blocklets which were of ~30 nm in size were visible in topographical images of all three starches. This is comparative to what is presented in the literature that have been reported to be of ~30 nm in mature corn, potato, rice, sweet potato and wheat starches (Ohtani & Yoshino, 2000) and of 10-50 nm in both large and small granules of mature wheat starch (Baldwin et al., 1998). These blocklets had organized into nodules on the surface of the granule and exhibited differences in their height (see arrows labelled as 'N' in Fig. 6). Furthermore, three dimensional structures of these substructures demonstrated a pointy shape in 28 DAP starch and a rounded shape in 17 DAP and 47 DAP starches (data not shown). This demonstrates different levels of organizations of glucan polymers on the surface of starch granules at different stages of maturities. Depressions were also observed in starches of all three maturities (see arrows labelled as 'D' in Fig. 6). Depressions and protrusions on the granule surfaces of wheat, triticale, maize, potato and tapioca starches have been previously observed (Juszczak, 2003; Juszczak et al., 2003a, 2003b). These depressions can be surface pores or the ends of penetrating channels (Juszczak et al., 2003a, 2003b). Furthermore, the

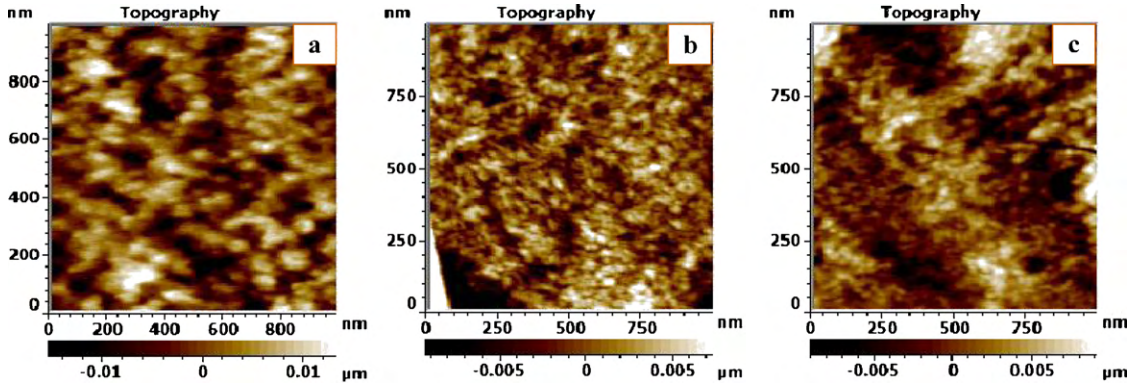

Fig. 7. Topographic AFM images of the surfaces of starches exposed to iodine vapor following equilibration to 0.97a_w. (a) 17 DAP; (b), 28 DAP; (c) 47 DAP. The scan size is 1 μm × 1 μm.

phase images of these starches demonstrated that there are some structures in the dark areas of topographical images that were not resolved.

Fig. 7 shows topographic images of iodine exposed starches of all three maturities. Iodine made the granule surface more crowded and it was clearly visible on the surface of 28 DAP starch granule. This crowding could be because of the complex formation of linear polymers or linear segments of branched polymers which were on the surface of the starch granule with iodine molecules. This was clearly seen in an in situ study on potato starch which was carried out in our laboratory (unpublished data; manuscript in review). Furthermore, round shaped nodules observed on the 17 DAP or 47 DAP starch granule surfaces became more pointy shaped after exposure to iodine. This transformation is likely because the linear polymers that were not rigid and did not lay down on the granule surface earlier had become rigid and stood up on the granule surface as a result of the formation of helical complexes with iodine. However, in the 28 DAP starch, iodine caused nodules to lose their pointy shape. The 28 DAP starch also behaved differently from the 17 DAP and 47 DAP starches in the K/S spectra. Furthermore, nodules which were on valleys were more visible after exposure to iodine. Lineback (1986), introduced the concept of the 'Hairy billiard ball' to describe the surface of the starch granule. He suggested that it is unlikely that starch granules have smooth surfaces since there are AM and AMP molecules of different lengths that are radially oriented within the granule. Later this concept was used to explain the enzyme degradation of the starch granule (Lynn & Stark, 1992; Stark & Lynn, 1992). Although our observations support the above concept, more intensive study is necessary before generalizing the observations.

4. Conclusion

Based on this research following conclusions could be obtained for hard red spring wheat starches at different stages of maturity. Iodine binding properties of starches at different stages of maturity were not similar. 28 DAP starch had the longest polymer chains available to bind with iodine even at moisture content as low as at $0.75a_w$, while 47 DAP starch had equal chain lengths (at $0.75a_w$) or shorter chains (at $0.97a_w$) than 28 DAP starch. Furthermore, the effect of iodine on the crystallinity ($\%RC_A$) of these starch granules increased with the maturity of starch. Iodine disrupted crystallites of these starches which were only at the boundary of order/disorder packing into completely disorder/amorphous state. Iodine further increased the contribution from single helices to the crystallinity (%RC). The morphology of 28 DAP starch was also different from the morphology of starch at the other two maturities. Interaction of iodine with starch polymers and its effect to the surface morphology were evidenced by AFM images. Different levels of interaction of iodine with starches equilibrated to the same a_w indicate that starches at different maturities have different architecture.

Acknowledgements

The authors thank Dr. D.E. Falk, Department of Plant Agriculture, University of Guelph, for providing seeds and Dr. A. Marangoni, Department of Food Science, University of Guelph, for providing access to X-ray instrument and helping in analysis. This research was funded by a Discovery grant from the National Science and Engineering Research Council of Canada.

Appendix A. Supplementary data

Supplementary data associated with this article can be found, in the online version, at doi:10.1016/j.carbpol.2010.05.053.

References

An, H. J., Yang, H. S., Liu, Z. D., & Zhang, Z. Z. (2008). Effects of heating modes and sources on nanostructure of gelatinized starch molecules using atomic force microscopy. *Lwt-Food Science and Technology*, *41*, 1466–1471.
Ayoub, A., Ohtani, T., & Sugiyama, S. (2006). Atomic force microscopy investigation of disorder process on rice starch granule surface. *Starch-Starke*, *58*, 475–479.
Baker, A. A., Miles, M. J., & Helbert, W. (2001). Internal structure of the starch granule revealed by AFM. *Carbohydrate Research*, *330*, 249–256.
Baldwin, P. M., Adler, J., Davies, M. C., & Melia, C. D. (1998). High resolution imaging of starch granule surfaces by atomic force microscopy. *Journal of Cereal Science*, *27*, 255–265.
Baldwin, P. M., Davies, M. C., & Melia, C. D. (1997). Starch granule surface imaging using low-voltage scanning electron microscopy and atomic force microscopy. *International Journal of Biological Macromolecules*, *21*, 103–107.
Banks, W., Greenwood, C. T., & Khan, K. M. (1971). The interaction of linear, amylose oligomers with iodine. *Carbohydrate Research*, *17*, 25–33.
Bates, L., French, D., & Rundle, R. E. (1943). Amylose and amylopectin content of starches determined by their iodine complex formation. *Journal of the American Chemical Society*, *65*, 142–148.
Bechtel, D. B., & Wilson, J. D. (2003). Amyloplast formation and starch granule development in hard red winter wheat. *Cereal Chemistry*, *80*, 175–183.
Bechtel, D. B., Zayas, I., Kaleikau, L., & Pomeranz, Y. (1990). Size-distribution of wheat-starch granules during endosperm development. *Cereal Chemistry*, *67*, 59–63.
Billmeyer, F. W., & Saltzman, M. (1981). The coloring of materials in industry. In F. W. Billmeyer, & M. Saltzman (Eds.), *Principles of color technology* (pp. 133–172). New York: Wiley.
Buleon, A., Veronese, G., & Putaux, J.-L. (2007). Self association and crystallization of amylose. *Australian Journal of Chemistry*, *60*, 706–718.
Cheetham, N. W. H., & Tao, L. (1998). Variation in crystalline type with amylose content in maize starch granules: An X-ray powder diffraction study. *Carbohydrate Polymers*, *36*, 277–284.
Chiang, P., Li, P., Huang, C., & Wang, C. R. (2007). Changes in functional characteristics of starch during water caltrop (Trapa Quadrispinosa Roxb.) growth. *Food Chemistry*, *104*, 376–382.
Chrastil, J. (1987). Improved colorimetric determination of amylose in starches or flours. *Carbohydrate Research*, *159*, 154–158.
Dang, J. M. C., Braet, F., & Copeland, L. (2006). Nanostructural analysis of starch components by atomic force microscopy. *Journal of Microscopy-Oxford*, *224*, 181–186.
Gallant, D. J., Bouchet, B., & Baldwin, P. M. (1997). Microscopy of starch: Evidence of a new level of granule organization. *Carbohydrate Polymers*, *32*, 177–191.
Gessler, K., Usón, I., Takaha, T., Krauss, N., Smith, S. M., Okada, S., et al. (1999). V-amylose at atomic resolution: X-ray structure of a cycloamylose with 26 glucose residues (cyclomaltohexaicosaose). *Proceedings of the National Academy of Sciences*, *96*, 4246–4251.
Gunning, A. P., Giardina, T. P., Faulds, C. B., Juge, N., Ring, S. G., Williamson, G., et al. (2002). Surfactant-mediated solubilisation of amylose and visualisation by atomic force microscopy. *Carbohydrate Polymers*, *51*, 177–182.
Hayashi, M., Kiribuchi-Otobe, C., & Seguchi, M. (2005). Ghosts of B-type wheat starch granules in concentrated KI/I_2 solution. *Starch/Starke*, *57*, 384–387.
Juszczak, L. (2003). Surface of triticale starch granules - NC-AFM observations. *Electronic Journal of Polish Agricultural Universities*, *6*
Juszczak, L., Fortuna, T., & Krok, F. (2003a). Non-contact atomic force microscopy of starch granules surface. Part I. Potato and tapioca starches. *Starch/Starke*, *55*, 1–7.
Juszczak, L., Fortuna, T., & Krok, F. (2003b). Non-contact atomic force microscopy of starch granules surface. Part II. Selected cereal starches. *Starch/Starke*, *55*, 8–16.
Kim, H.-S., & Huber, K. C. (2008). Channels within soft wheat starch A- and B-type granules. *Journal of Cereal Science*, *48*, 159–172.
Kulp, K., & Mattern, P. J. (1973). Some properties of starches derived from wheat of varied maturity. *Cereal Chemistry*, *50*, 496–504.
Kuntson, C. A., Jr., Cluskey, J. E., & Dintzis, F. R. (1982). Properties of amylose-iodine complexes prepared in the presence of excess iodine. *Carbohydrate Research*, *101*, 117–128.
Langeveld, S. M. J., Van Wijk, R., Stuurman, N., Kijne, J. W., & de Pater, S. (2000). B-type granule containing protrusions and interconnections between amyloplasts in developing wheat endosperm revealed by transmission electron microscopy and GFP expression. *Journal of Experimental Botany*, *51*, 1357–1361.
Lineback, D. R. (1986). Current concepts of starch structure and its impact on properties. *Journal of the Japanese Society of Starch Science*, *33*, 80–88.
Liu, Z. D., Chen, S. F., Ouyang, Z. Q., Guo, Y. C., Hu, J., & Li, M. Q. (2001). Study on the chain structure of starch molecules by atomic force microscopy. *Journal of Vaccum Science & Technology*, *19*, 111–114.
Liu, Q., Weber, E., Currie, V., & Yada, R. (2003). Physicochemical properties of starches during potato growth. *Carbohydrate Polymers*, *51*, 213–221.
Lopez-Rubio, A., Flanagan, B. M., Gilbert, E. P., & Gidley, M. J. (2008). A novel approach for calculating starch crystallinity and its correlation with double helical content: A combine XRD and NMR study. *Biopolymers*, *89*, 761–768.
Lynn, A., & Stark, J. R. (1992). The action of isoamylase on the surface of starch granules. *Carbohydrate Research*, *227*, 379–383.
McDonald, A. M. L., Stark, J. R., Morrison, W. R., & Ellis, R. P. (1991). The composition of starch granules from developing barley genotypes. *Journal of Cereal Science*, *13*, 93–112.
Morris, V. J., Gunning, A. P., Faulds, C. B., Williamson, G., & Svensson, B. (2005). AFM images of complexes between amylose and Aspergillus niger glucoamylase

mutants, native, and mutant starch binding domains: A model for the action of glucoamylase. *Starch/Starke*, *57*, 1–7.
Morrison, W. R. (1988). Lipids in cereal starches: A review. *Journal of Cereal Science*, *8*, 1–15.
Morrison, W. R., & Gadan, H. (1987). The amylose and lipid contents of starch granules in developing wheat endosperm. *Journal of Cereal Science*, *5*, 263–275.
Murdoch, K. A. (1992). The amylose-iodine complex. *Carbohydrate Research*, *233*, 161–174.
Nimz, O., Geßler, K., Usón, I., Laettig, S., Welfle, H., Sheldrick, G. M., et al. (2003). X-ray structure of the cyclomaltohexaicosaose triiodide inclusion complex provides a model for amylose-iodine at atomic resolution. *Carbohydrate Research*, *338*, 977–986.
Ohtani, T., & Yoshino, T. (2000). High-resolution imaging of starch granule structure using atomic force microscopy. *Starch/Starke*, *52*, 150–153.
Ohtani, T., Yoshino, T., Ushiki, T., Hagiwara, S., & Maekawa, T. (2000). Structure of rice starch granules in nanometre scare as revealed by atomic force microscopy. *Journal of Electron Microscopy*, *49*, 487–489.
Park, S. H., Bean, S. R., Wilson, J. D., & Schober, T. J. (2006). Rapid isolation of sorghum and other cereal starches using sonication. *Cereal Chemistry*, *83*, 611–616.
Peng, M., Gao, M., Abdel-Aal, E. S. M., Hucl, P., & Chibbar, R. N. (1999). Separation and characterization of A- and B-type starch granules in wheat endosperm. *Cereal Chemistry*, *76*, 375–379.
Rendleman, J. A. (2003). The reaction of starch with iodine vapor. Determination of iodide-ion content of starch–iodine complexes. *Carbohydrate Polymers*, *51*, 191–202.
Ridout, M. J., Gunning, A. P., Parker, M. L., Wilson, R. H., & Morris, V. J. (2002). Using AFM to image the internal structure of starch granules. *Carbohydrate Polymers*, *50*, 123–132.
Ridout, M. J., Parker, M. L., Hedley, C. L., Bogracheva, T. Y., & Morris, V. J. (2004). Atomic force microscopy of pea starch: Origins of image contrast. *Biomacromolecules*, *5*, 1519–1527.
Rundle, R. E., & Baldwin, R. R. (1943). The configuration of starch and the starch–iodine complex. The dichroism of flow of starch–iodine solutions. *Journal of the American Chemical Society*, *65*, 554–558.
Rundle, R. E., & Edwards, F. C. (1943). The configuration of starch in the starch–iodine complex. IV. An X-ray diffraction investigation of butanol precipitated amylose. *Journal of the American Chemical Society*, *65*, 2200–2203.
Rundle, R. E., & French, D. (1943a). The configuration of starch and the starch–iodine complex. II. Optical properties of crystalline starch fractions. *Journal of the American Chemical Society*, *65*, 558–561.
Rundle, R. E., & French, D. (1943b). The configuration of starch and the starch–iodine complex. III. X-ray diffraction studies of the starch–iodine complex. *Journal of the American Chemical Society*, *65*, 1707–1710.
Saibene, D., & Seetharaman, K. (2006). Segmental mobility of polymers in starch granules at low moisture contents. *Carbohydrate Polymers*, *64*, 539–547.
Saibene, D., Zobel, H. F., Thompson, D. B., & Seetharaman, K. (2008). Iodine-binding in granular starch: Different effects of moisture content for corn and potato starch. *Starch/Starke*, *60*, 165–173.
Sevenou, O., Hill, S. E., Farhat, I. A., & Mitchell, J. R. (2002). Organization of the external region of the starch granule as determined by infrared spectroscopy. *International Journal of Biological Macromolecules*, *31*, 79–85.
Simonne, A. H., Simonne, E. H., Eitenmiller, R. R., Mills, H. A., & Cresman, C. P. (1997). Could the Dumas method replace the Kjeldhal digestion for nitrogen and crude protein determination in foods? *Journal of the Science of Food and Agriculture*, *73*, 39–45.
Stark, J. R., & Lynn, A. (1992). Biochemistry of plant polysaccharides: starch granules large and small. *Biochemical Society Transactions*, *20*, 7–12.
Stevenson, D. G., Jane, J., & Inglett, G. E. (2007). Structures and physicochemical properties of starch from immature seeds of soybean varieties (Glycinemax (L.) Merr.) exhibiting normal, low-linolenic or low-saturated fatty acid oil profiles at maturity. *Carbohydrate Polymers*, *70*, 149–159.
Suryanarayana, C., & Norton, M. G. (1998). Practical aspects of X-ray diffraction. In C. Suryanarayana, & M. G. Norton (Eds.), *X-ray diffraction: A practical approach* (pp. 63–94). NY: Plenum Press.
Szymonska, J., & Krok, F. (2003). Potato starch granule nanostructure studied by high resolution non-contact AFM. *International Journal of Biological Macromolecules*, *33*, 1–7.
Tang, C. M., & Copeland, L. (2007). Investigation of starch retrogradation using atomic force microscopy. *Carbohydrate Polymers*, *70*, 1–7.
Teitelbaum, R. C., Ruby, S. L., & Marks, T. J. (1980). A resonance Raman/iodine Mössbauer investigation of starch–iodine structure. Aqueous solution and iodine vapour preparations. *Journal of the American Chemical Society*, *102*, 3322–3328.
Thoma, J. A., & French, D. (1960). The starch-iodine-iodide interaction. Part I. Spectrophotometric investigations. *Journal of the American Chemical Society*, *82*, 4144–4147.
Thomson, N. H., Miles, M. J., Ring, S. G., Shewry, P. R., & Tatham, A. S. (1994). Real-time imaging of enzymatic degradation of starch granules by atomic-force microscopy. *Journal of Vacuum Science & Technology, B*, *12*, 1565–1568.